Observation of quasi-coherent edge fluctuations in Ohmic plasmas on National Spherical Torus Experiment

Santanu Banerjee, A. Diallo, and S. J. Zweben

Citation: Physics of Plasmas **23**, 044502 (2016); doi: 10.1063/1.4946871
View online: http://dx.doi.org/10.1063/1.4946871
View Table of Contents: http://scitation.aip.org/content/aip/journal/pop/23/4?ver=pdfcov
Published by the AIP Publishing

Observation of quasi-coherent edge fluctuations in Ohmic plasmas on National Spherical Torus Experiment

Santanu Banerjee,[1] A. Diallo,[2] and S. J. Zweben[2]
[1]Institute for Plasma Research, Bhat, Gandhinagar 382428, Gujarat, India
[2]Princeton Plasma Physics Laboratory, Princeton, New Jersey 08540, USA

(Received 12 February 2016; accepted 3 April 2016; published online 20 April 2016)

A quasi-coherent edge density mode with frequency $f_{mode} \sim 40$ kHz is observed in Ohmic plasmas in National Spherical Torus Experiment using the gas puff imaging diagnostic. This mode is located predominantly just inside the separatrix, with a maximum fluctuation amplitude significantly higher than that of the broadband turbulence in the same frequency range. The quasi-coherent mode has a poloidal wavelength $\lambda_{pol} \sim 16$ cm and a poloidal phase velocity of $V_{pol} \sim 4.9 \pm 0.3$ km s^{-1} in the electron diamagnetic direction, which are similar to the characteristics expected from a linear drift-wave-like mode in the edge. This is the first observation of a quasi-coherent edge mode in an Ohmic diverted tokamak, and so may be useful for validating tokamak edge turbulence codes. *Published by AIP Publishing*. [http://dx.doi.org/10.1063/1.4946871]

Edge turbulence appears to be a ubiquitous feature of magnetic confinement devices and can affect the overall quality of the discharge performance, as seen in the better confinement in H-mode associated with reduced edge turbulence levels. Normally, edge turbulence in tokamaks is dominated by broadband density fluctuations with a wide frequency and wavelength spectrum ($f \sim 1$ kHz to 1 MHz and $\lambda_{pol} \sim 0.1$ cm to 10 cm), without any significant coherent modes associated with the underlying linear instabilities. These observations are generally consistent with the broadband spectra seen in computational simulations of the nonlinear evolution of drift-like modes. Note that, here, we are focusing on density fluctuations (i.e., electrostatic modes), and not on edge magnetic fluctuations such as kink or tearing modes or edge localized modes (ELM).

Despite the usual dominance of broadband incoherent turbulence in the edge, there have been several previous observations of near-coherent electrostatic edge modes in tokamaks. A "quasi-coherent" mode (QCM) was first observed in H-mode plasmas in Princeton Divertor Experiment tokamak using CO_2 and microwave scattering,[1] and studies of this type of quasi-coherent mode in the edge of H-mode plasmas have continued until the present day, for example, in Alcator C-Mod,[2–4] EAST,[5] and DIII-D.[6] For example, a QCM in C-Mod at ~100 kHz produces strong outward particle transport in the edge region during the enhanced D alpha H-mode regime, which limits the pedestal growth and eliminates the usual ELMS,[2] and quasi-coherent fluctuations in DIII-D at ~100 kHz plays a role in the inter-ELM dynamics and tracks the evolution of the H-mode temperature gradient in the pedestal.[6] A potentially different type of quasi-coherent mode was observed in Ohmic (non-H-mode) plasmas in the Texas Experimental Tokamak (TEXT) using Langmuir probes and a heavy ion beam probe.[7] This mode was localized at $r/a \sim 0.95$ and had a frequency of $f \sim 20$ kHz, a poloidal wavenumber of $k_{pol} \sim 50$ m^{-1}, and propagated in the electron diamagnetic direction. Quasi-coherent modes have also been observed in the core of several tokamaks using microwave reflectometry, and identified with trapped electron modes.[8]

The present paper describes observations of a previously undetected quasi-coherent drift-like mode in the edge of Ohmic plasmas in National Spherical Torus Experiment (NSTX),[9] a mid-sized spherical tokamak. These measurements were made using a gas puff imaging (GPI) diagnostic, which has previously been used to characterize the variations in broadband edge turbulence seen in a wide database of NSTX shots,[10] including those analyzed in the present paper. This is the first observation of a quasi-coherent edge mode in an Ohmic diverted tokamak, and so may be useful for validating tokamak edge turbulence codes.

Although no previous observations of a quasi-coherent edge density fluctuations have been reported in NSTX in Ohmic discharges, a largely magnetic edge harmonic oscillation (EHO) was observed during ELM-free H-mode discharges,[11] although this was very small in amplitude and had no measurable effect on the edge profiles. Also, a near-coherent oscillation at ~3 kHz in edge poloidal velocity (along with some modulation of density) was seen previously with GPI in NSTX, and tentatively identified as a geodesic acoustic mode (GAM).[12]

The NSTX GPI diagnostic used for this paper measures the D_α line emission from a deuterium gas puff near the outer mid-plane edge with a camera view aligned along the local B field to resolve the 2-D radial vs. poloidal structure of the edge turbulence.[10] Images are acquired at ~400 000 frames per second using an 80×64 pixel array with 12 bit dynamic range. The discharges analyzed in this work are purely Ohmic lower-single null diverted deuterium plasmas (#141741–141756), with plasma current $I_p = 0.8$ MA and toroidal field $B_t = 0.35$–0.40 T, and an outer gap from the separatrix to the wall of ~9 cm. An Ohmic H mode transition has been observed in about half of the shots in this series, while the rest remained in Ohmic "L-mode" all through the GPI time window. For this paper, we focus on the quasi-coherent mode activity in the L-mode phase of these Ohmic plasmas. Density (n_e) and temperature (T_e) profiles were measured by Thomson scattering near the GPI peak time (i.e., in L-mode), showing that the edge n_e and T_e at ~5 cm inside the separatrix were

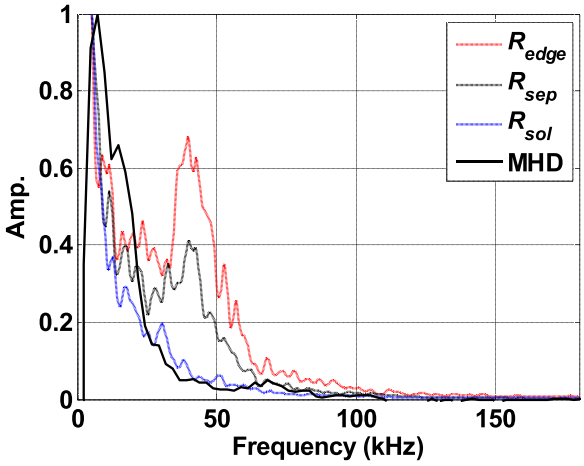

FIG. 1. Frequency spectra of the GPI signal amplitude $\tilde{I}$ at three radial locations R_{edge}, R_{sep}, and R_{sol}, respectively, are shown in L-mode for a representative shot (#141754). A distinct peak can be seen at R_{edge} and R_{sep} at ~40 kHz, while no such peak is apparent at R_{sol} or in the magnetic loop (MHD) signal.

$\sim 0.9 \times 10^{13}\,\mathrm{cm}^{-3}$ and 60 eV; further information on these Ohmic discharges is shown in Table 2 of Ref. 10.

The measured GPI light intensity fluctuations $\tilde{I}$ are mainly due to electron density fluctuations in the edge and scape-off layer (SOL) of Ohmic discharges in NSTX. For use in the GPI analysis below, three radial regions are defined as follows: R_{edge} (−4 to −5 cm inside the separatrix), R_{sep} (near the separatrix position), and R_{sol} (in the SOL at 3 to 4 cm outside the separatrix). The frequency spectra of the amplitude of the fluctuations in $\tilde{I}$ for the three radial zones are shown in Fig. 1 for a representative shot during the L-mode time period (208–218 ms). Here, the amplitude scale is in relative units for each signal (normalized to 1 at the lowest frequency), since the absolute value of the GPI signals is not relevant for estimating the local fluctuation level, because the D_α brightness depends on the local density and temperature and the strength of the GPI gas puff. The most significant part of Fig. 1 is the shape of the frequency spectrum for each signal. A clear spectral peak can be seen in the R_{edge} and R_{sep} regions at ~40 kHz, but no such peaks are apparent in the scrape-off region at R_{sol}, as indicated in Fig. 1. There is also no such peak at this frequency visible in the nearby magnetic loop (MHD) signal, also shown in Fig. 1. The quasi-coherent mode amplitude at R_{edge} and R_{sep} in Fig. 1 is ~85% and ~68% above the background broadband fluctuation level, as fit by a polynomial across the nearby frequency range.

The time dependence of the quasi-coherent mode is illustrated by the spectrogram of the GPI intensity $\tilde{I}$ in Fig. 2 for R_{edge} and R_{sep} for two representative shots. Shot 141754 is a pure Ohmic L-mode shot, while 141751 has a L-H transition later at 235.3 ms. Both shots show a fairly clear spectral peak in the R_{edge} and R_{sep} regions at ~40 kHz, but no such peaks are apparent at R_{sol}. The quasi-coherent mode appears in L-mode of all the shots of this series including the shots with an L-H transition later on, although the amplitude of the quasi-coherent mode appears to decrease ~100–150 ms before the L-H transition, as shown for shot 141751 in Fig. 2. The exact physical mechanism (e.g., flow shear) that can extinguish this mode prior to the L-H transition needs further investigation and will be reported in future.

The spatial structure of this quasi-coherent mode was investigated using the squared coherence (C) of $\tilde{I}$ evaluated between points separated in the radial and poloidal directions, given by

$$C_{\rho ref,\rho}(f) = \frac{|P_{\rho ref,\rho}(f)|^2}{P_{\rho ref,\rho ref}(f) P_{\rho,\rho}(f)}, \tag{1}$$

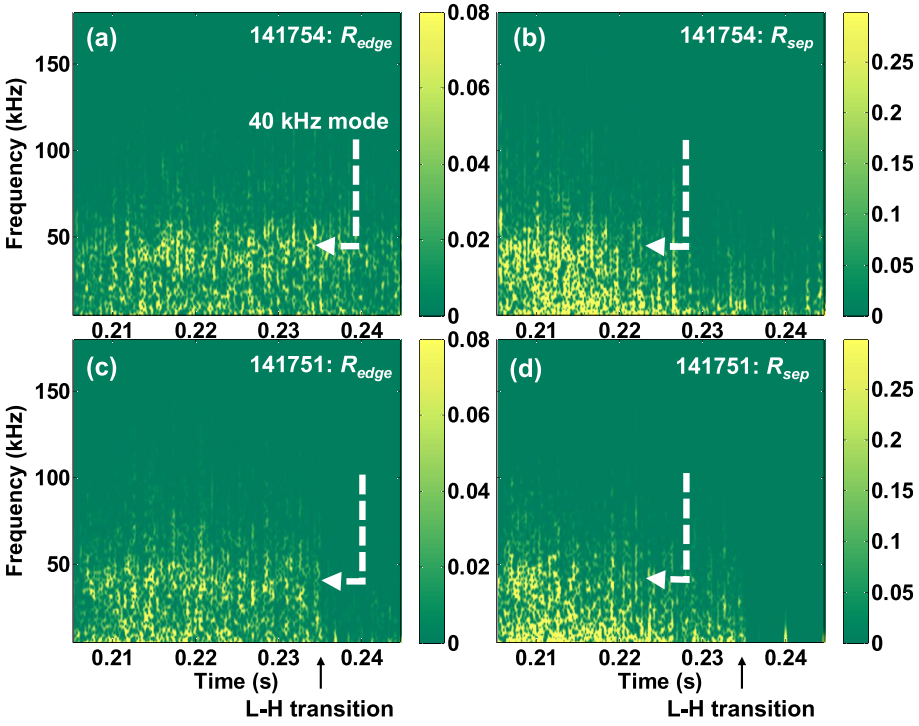

FIG. 2. (a) and (b) Spectrograms for the amplitude of $\tilde{I}$ fluctuations at R_{edge} and R_{sep} for the L-mode shot #141754, plotted with a linear color scale; (c) and (d) Same as the top row, but for the shot #141751 having a L-H transition at 235.3 ms. Frequency scale spans from 5 kHz to 180 kHz. The QCM amplitude falls monotonically with time during L-mode of all shots and well before the transition in L-H transition shots. White arrows show the QCM frequency.

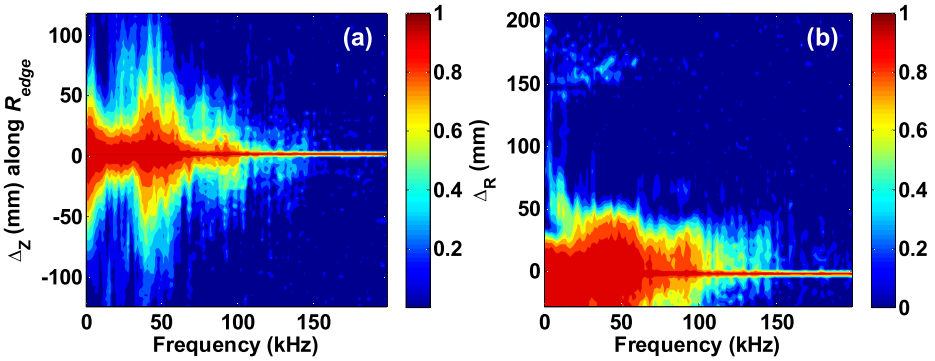

FIG. 3. (a) Cross-coherence along the poloidal direction at R_{edge} with the reference pixel at $R = R_{edge}$ and $Z = 20$ cm; (b) same along the radial direction.

where ($P\rho_{ref},\rho_{ref}(f)$ and $P\rho,\rho(f)$) are power spectral densities of a reference pixel (ρ_{ref}) and any other pixel ($\rho = [R,Z]$), and ($P\rho_{ref},\rho(f)$) is the cross power spectral density.

Fig. 3(a) shows the cross-coherence in the poloidal direction for a reference pixel at the middle of the GPI image ($Z = 20$ cm above mid-plane) at a radius R_{edge}. The poloidal coherence length (i.e., the FWHM of the poloidal cross-correlation function) at the quasi-coherent mode frequency of ~40 kHz is ~16 cm, which is larger than the coherence length of the broadband turbulence at higher and lower frequencies. The radial cross-coherence from the same pixel is shown in Fig. 3(b), with a radial coherence length at ~40 kHz of ~10 cm (FWHM), which is slightly larger than at other frequencies.

A two-dimensional discrete Fourier transform (DFT) estimate of the poloidal wavenumber-frequency (k_z–f) spectra for fluctuations in the edge region R_{edge} is shown for shot 141754 (pure Ohmic L-mode) in Fig. 4. Inside the separatrix, the k_z–f spectra show dominance of fluctuation propagation in the electron diamagnetic drift direction (EDD) in the laboratory frame. The quasi-coherent mode feature is marked by the arrow at ~40 kHz. For this case, the poloidal wave number is $k_{pol} \sim 40\ \mathrm{m}^{-1}$ such that the poloidal wavelength is $\lambda_{pol} \sim 15.7$ cm, similar to the length found from the coherence analysis of Fig. 3. The poloidal velocity of this mode (and also the broadband turbulence) is $V_{pol} = 4.9 \pm 0.28\ \mathrm{km\ s}^{-1}$ in the laboratory frame. The V_{pol} of the broadband turbulence evaluated for the SOL region is in the opposite (ion diamagnetic drift, IDD) direction.[10]

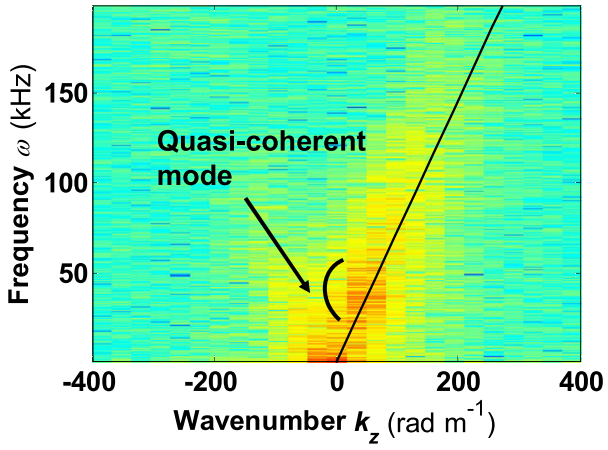

FIG. 4. Two-dimensional poloidal wavenumber-frequency (k_z-f) spectra at R_{edge} during L-mode (#141754). $k_z > 0$ corresponds to propagation in the EDD. The coherent mode can be seen at ~40 kHz as shown by the black arrow. Black solid line is the linear fit for poloidal velocity.

Several features of the time evolution of the quasi-coherent mode are shown in Fig. 5. Fig. 5(a) shows variation of the mean GPI signal level in the entire GPI frame for the representative shot (#141751) featuring L-H transition at 235.3 ms. The intensity level follows the GPI gas puffing, peaking at ~213 ms and decreasing over time. Fig. 5(b) shows the magnetic fluctuation spectrogram obtained from the Mirnov coil on the outer wall closest to the GPI view, showing the absence of any quasi-coherent mode near 40 kHz (black arrow). Hence, the mode is predominantly electrostatic; however, a weak magnetic signature due to potential high n-mode nature cannot be ruled out. Figure 5(c) shows the GPI spectrum at R_{edge}, with a white arrow near quasi-coherent mode frequency of 40 kHz. Figures 5(d) and 5(e) show the radial and poloidal distributions of the GPI fluctuation amplitude in the 35–45 kHz frequency range at $Z = 20$ cm and R_{edge}, respectively. The quasi-coherent mode has a radial peak location within ~0–5 cm inside the separatrix, but distributed over ~10–20 cm in the poloidal direction.

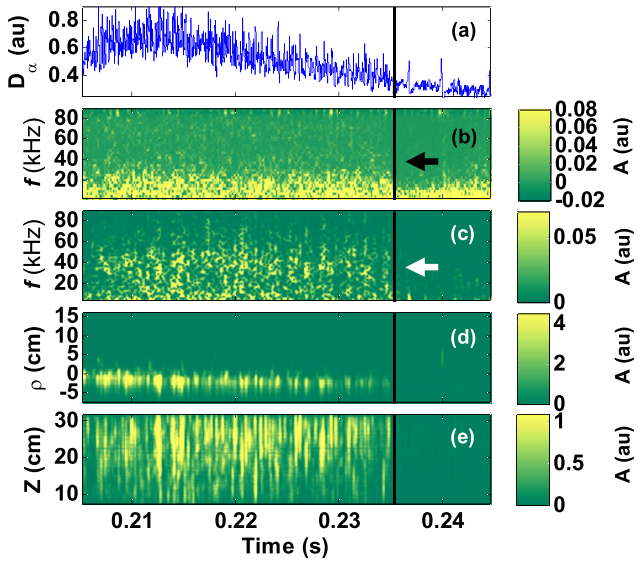

FIG. 5. Time evolution of (a) the mean GPI intensity, (b) frequency spectrum of nearby magnetic fluctuations, (c) frequency spectrum of GPI fluctuation at R_{edge}, with black and white arrows in the frequency range of the quasi-coherent mode (#141751). The L-H transition is indicated by the solid black vertical line. Parts (d) and (e) show the radial and poloidal distributions of the spectral amplitude in the mode frequency range (35–45 kHz).

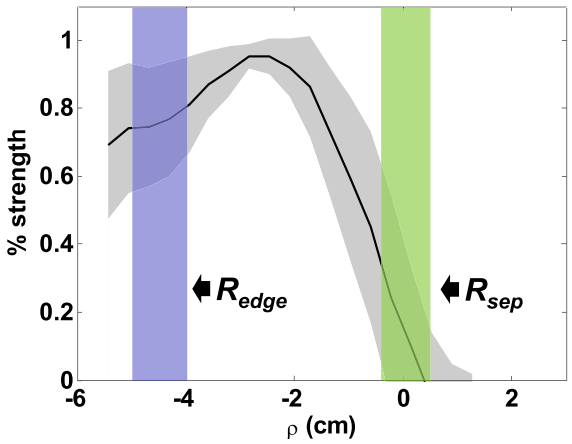

FIG. 6. Radial profile of the relative amplitude of the quasi-coherent mode above the broadband fluctuation level.

Fig. 6 shows radial profiles of the relative amplitude of the quasi-coherent mode during the L-mode period averaged over all shots in this series. The amplitude shown is the fractional level of the quasi-coherent mode above the broadband spectrum in this frequency range. The mode amplitude peaks between R_{edge} and R_{sep} at about 2–3 cm inside the separatrix, with a scatter shown by the gray shaded region. The mode frequency is between 35 and 40 kHz, with no clear variation of frequency vs. radius in this radial region.

The characteristics of the quasi-coherent mode described in this brief communication can be compared with generic estimates for the drift-wave-like modes in the edge of these plasmas. At a radius of 2 cm inside the separatrix in these Ohmic discharges (#141741–56 at ~213 ms), the average Thomson scattering data give $T_e \sim 23 \pm 4$ eV, so the drift-wave gyroradius (at the electron temperature) is $\rho_s \sim 0.4$ cm using the edge toroidal magnetic field. Thus, the normalized mode size scale using the measured $k_{pol} \sim 40\,\mathrm{m}^{-1}$ is $k_{pol}\rho_s \sim 0.15$, which is qualitatively consistent with the drift-wave size scale of typically $k_{pol}\rho_s \sim 0.2$.[13] The measured density gradient scale length at this radius is $L_n \sim 4 \pm 2$ cm, and the sound speed is $c_s = 3.4 \times 10^6\,\mathrm{cm\ s}^{-1}$ (for deuterium). Thus, the expected drift-wave phase velocity (electron diamagnetic speed) is $V_{e*} = c_s\rho_s/L_n \sim 3.4\,\mathrm{km\ s}^{-1}$, which is consistent with the observed wave speed of $V_{pol} \sim 4.9\,\mathrm{km\ s}^{-1}$. Thus, we tentatively identify the observed quasi-coherent mode as a generic drift-wave-like mode or resonance, although the precise instability mechanism and damping mechanism cannot be determined from this data, and we have no clear explanation for the observed width of the mode.

In summary, we have discovered a quasi-coherent mode existing within the broadband spectrum of fluctuations in the edge region of NSTX Ohmic plasmas. This mode is similar to the quasi-coherent mode described previously for a circular, limited Ohmic plasma in the TEXT tokamak,[7] and also similar to the quasi-coherent modes recently seen in H-mode plasmas in C-Mod,[2–4] EAST,[5] and DIII-D.[6] The relative fluctuation level of this quasi-coherent mode at 35–45 kHz in NSTX is significantly higher than that of the background turbulence, so this mode might be viewed as a remnant of the linear instability which is responsible for the nonlinear turbulence. For example, recent Scrape Off Layer Turbulence simulations[14] show some coherent interchange mode structure underlying edge turbulence in NSTX. The present paper described the first observation of a quasi-coherent edge mode in an Ohmic diverted tokamak, and so may be useful for validating such edge turbulence codes.

Support and contributions from N. Crocker, E. Fredrickson, S. Kaye, S. Kubota, B. LeBlanc, R. Maingi, R. Maqueda, T. Munsat, S. Sabbagh, Y. Sechrest, J. R. Myra, D. A. Russell, and the National Spherical Torus Experiment Team are gratefully acknowledged. One of the authors (S.B.) would also like to thank H. Zushi and J. Ghosh for many useful discussions during the course of this work. This work was supported by U.S. DOE Contract DE-AC02-09CH11466. The digital data for this paper can be found at http://arks.princeton.edu/ark:/88435/dsp0170795b055.

[1]R. E. Slusher, C. M. Surko, J. F. Valley, T. Trowley, E. Mazzucato, and K. McGuire, Phys. Rev. Lett. **53**, 667 (1984).
[2]B. LaBombard, T. Golfinopoulos, J. L. Terry, D. Brunner, E. Davis, M. Greenwald, J. W. Hughes, and Alcator C-Mod Team, Phys. Plasmas **21**, 056108 (2014).
[3]A. Diallo, J. W. Hughes, S.-G. Baek, B. LaBombard, J. Terry, I. Cziegler, A. Hubbard, E. Davis, J. Walk, L. Delgado-Aparicio, M. L. Reinke, C. Theiler, R. M. Churchill, E. M. Edlund, J. Canik, P. Snyder, M. Greenwald, A. White, and the Alcator C-Mod Team, Nucl. Fusion **55**, 053003 (2015).
[4]A. Diallo, J. W. Hughes, M. Greenwald, B. LaBombard, E. Davis, S-G. Baek, C. Theiler, P. Snyder, J. Canik, J. Walk, T. Golfinopoulos, J. Terry, M. Churchill, A. Hubbard, M. Porkolab, L. Delgado-Aparicio, M.L. Reinke, A. White, and Alcator C-Mod Team, Phys. Rev. Lett. **112**, 115001 (2014).
[5]H. Q. Wang, G. S. Xu, B. N. Wan, S. Y. Ding, H. Y. Guo, L. M. Shao, S. C. Liu, X. Q. Xu, E. Wang, N. Yan, V. Naulin, A. H. Nielsen, J. Juul Rasmussen, J. Candy, R. Bravenec, Y. W. Sun, T. H. Shi, Y. F. Liang, R. Chen, W. Zhang, L. Wang, L. Chen, N. Zhao, Y. L. Li, Y. L. Liu, G. H. Hu, and X. Z. Gong, Phys. Rev. Lett. **112**, 185004 (2014).
[6]A. Diallo, R. J. Groebner, T. L. Rhodes, D. J. Battaglia, D. R. Smith, T. H. Osborne, J. M. Canik, W. Guttenfelder, and P. B. Snyder, Phys. Plasmas **22**, 056111 (2015).
[7]H. Y. W. Tsui, P. M. Schoch, and A. J. Wootton, Phys. Fluids B **5**, 1274 (1993).
[8]H. Arnichand, R. Sabot, S. Hacquin, A. Krämer-Flecken, C. Bourdelle, J. Citrin, X. Garbet, J. C. Giacalone, R. Guirlet, J. C. Hillesheim, L. Meneses, and JET Contributors, Nucl. Fusion **55**, 093021 (2015).
[9]S. M. Kaye, T. Abrams, J.-W. Ahn, J. P. Allain, R. Andre, D. Andruczyk, R. Barchfeld, D. Battaglia, A. Bhattacharjee, F. Bedoya *et al.*, Nucl. Fusion **55**, 104002 (2015).
[10]S. J. Zweben, W. M. Davis, R. E. Bell, B. P. LeBlanc, S. M. Kaye, R. J. Maqueda, T. Munsat, J. R. Myra, Y. Sechrest, D. P. Stotler, and the NSTX Team, Nucl. Fusion **55**, 093035 (2015).
[11]J. K. Park, R. E. Bell, S. M. Kaye, W. M. Solomon, B. P. LeBlanc, A. Diallo, J. E. Menard, S. Kubota, and the NSTX Research Team, Nucl. Fusion **53**, 063012 (2013).
[12]Y. Sechrest, T. Munsat, D. A. D'Ippolito, R. J. Maqueda, J. R. Myra, D. R. Russell, and S. J. Zweben, Phys. Plasmas **18**, 012502 (2011).
[13]B. D. Scott, Phys. Plasmas **12**, 062314 (2005).
[14]D. A. Russell, D. A. D'Ippolito, J. R. Myra, J. M. Canik, T. K. Gray, and S. J. Zweben, Phys. Plasmas **22**, 092311 (2015).